

Kinetics and Mechanism of the Interaction of Nitric Oxide with Pentacyanoferrate(II). Formation and Dissociation of $[\text{Fe}(\text{CN})_5\text{NO}]^{3-}$ Federico Roncaroli,^{†,‡} José A. Olabe,^{*,‡} and Rudi van Eldik^{*,†}

Institute for Inorganic Chemistry, University of Erlangen-Nürnberg, Egerlandstrasse 1, 91058 Erlangen, Germany, and Department of Inorganic, Analytical and Physical Chemistry, INQUIMAE, Faculty of Exact and Natural Sciences, University of Buenos Aires, C1428EHA Buenos Aires, Argentina

Received February 26, 2003

The interaction of NO with $[\text{Fe}(\text{CN})_5\text{H}_2\text{O}]^{3-}$ (generated by aquation of the corresponding ammine complex) to produce $[\text{Fe}(\text{CN})_5\text{NO}]^{3-}$ was studied by UV–vis spectrophotometry. The reaction product is the well characterized nitrosyl complex, described as a low-spin Fe(II) bound to the NO radical. The experiments were performed in the pH range 4–10, at different concentrations of NO, temperatures and pressures. The rate law was first-order in each of the reactants, with the specific complex-formation rate constant, $k_f = 250 \pm 10 \text{ M}^{-1} \text{ s}^{-1}$ (25.4 °C, $I = 0.1 \text{ M}$, pH 7.0), $\Delta H_f^\ddagger = 70 \pm 1 \text{ kJ mol}^{-1}$, $\Delta S_f^\ddagger = +34 \pm 4 \text{ J K}^{-1} \text{ mol}^{-1}$, and $\Delta V_f^\ddagger = +17.4 \pm 0.3 \text{ cm}^3 \text{ mol}^{-1}$. These values support a dissociative mechanism, with rate-controlling dissociation of coordinated water, and subsequent fast coordination of NO. The complex-formation process depends on pH, indicating that the initial product $[\text{Fe}(\text{CN})_5\text{NO}]^{3-}$ is unstable, with a faster decomposition rate at lower pH. The decomposition process is associated with release of cyanide, further reaction of NO with $[\text{Fe}(\text{CN})_4\text{NO}]^{2-}$, and formation of nitroprusside and other unknown products. The decomposition can be prevented by addition of free cyanide to the solutions, enabling a study of the dissociation process of NO from $[\text{Fe}(\text{CN})_5\text{NO}]^{3-}$. Cyanide also acts as a scavenger for the $[\text{Fe}(\text{CN})_5]^{3-}$ intermediate, giving $[\text{Fe}(\text{CN})_6]^{4-}$ as a final product. From the first-order behavior, the dissociation rate constant was obtained as $k_d = (1.58 \pm 0.06) \times 10^{-5} \text{ s}^{-1}$ at 25.0 °C, $I = 0.1 \text{ M}$, and pH 10.2. Activation parameters were found to be $\Delta H_d^\ddagger = 106.4 \pm 0.8 \text{ kJ mol}^{-1}$, $\Delta S_d^\ddagger = +20 \pm 2 \text{ J K}^{-1} \text{ mol}^{-1}$, and $\Delta V_d^\ddagger = +7.1 \pm 0.2 \text{ cm}^3 \text{ mol}^{-1}$, which are all in line with a dissociative mechanism. The low value of k_d as compared to values for the release of other ligands L from $[\text{Fe}^{\text{II}}(\text{CN})_5\text{L}]^{n-}$ suggests a moderate to strong σ – π interaction of NO with the iron(II) center. It is concluded that the release of NO from nitroprusside in biological media does not originate from $[\text{Fe}(\text{CN})_5\text{NO}]^{3-}$ produced on reduction of nitroprusside but probably proceeds through the release of cyanide and further reactions of the $[\text{Fe}(\text{CN})_4\text{NO}]^{2-}$ ion.

Introduction

The chemistry of nitric oxide (NO) complexes has long been of interest to transition metal chemists and has been comprehensively reviewed.¹ It has seen a great revival since the discovery of NO as an essential biological molecule, with multiple physiological roles as a vascular regulator, as a

messenger in neuronal communication, and as a macrophage defense weapon.² The widely recognized clinical use of $[\text{Fe}(\text{CN})_5\text{NO}]^{2-}$ (nitroprusside, NP) as a potent hypotensive agent spans four decades, but the attribution of its pharmacological effect to the release of NO to the biological medium is more recent. It is assumed that the release is preceded by the reduction of coordinated NO^+ in NP, effected by biologically relevant thiolates.³ This raises a question on some unraveled kinetic properties of the $[\text{Fe}(\text{CN})_5\text{NO}]^{3-}$ ion.

* To whom correspondence should be addressed. E-mail: vaneldik@chemie.uni-erlangen.de (R.v.E.); olabe@qi.fcen.uba.ar (J.A.O.).

[†] University of Erlangen-Nürnberg.

[‡] University of Buenos Aires.

(1) (a) Richter-Addo, G. B.; Legzdins, P. *Metal Nitrosyls*; Oxford University Press: New York, 1992. (b) Special issue devoted to nitric oxide chemistry: Richter-Addo, G. B.; Legzdins, P.; Burstyn, J. N., Guest Eds., *Chem. Rev.* **2002**, 102, 861–1270. (c) Mingos, D. M. P.; Sherman, D. J. *Adv. Inorg. Chem.* **1989**, 34, 293–377.

(2) (a) Feelish, M.; Stamler, J. S., Eds. *Methods in Nitric Oxide Research*; Wiley: Chichester, England, 1996 and references therein. (b) *Nitric Oxide, Principles and Actions*; Lancaster, J., Jr., Ed.; Academic Press: New York, 1996. (c) Butler, A. R.; Williams, D. L. H. *Chem. Soc. Rev.* **1993**, 22, 233–241.

In general, the mechanistic details on the coordination of NO to transition metal centers, as well as its further dissociation reactions, have been insufficiently disclosed.⁴ This is probably related to the difficulties in the handling of NO solutions free of oxidizing impurities. More recent work, particularly focused on the reactions of NO with porphyrin-based molecules,^{4,5} has given a great impulse to these studies. In the case of classical coordination compounds, several families of nitrosyl complexes of the type $\{X_5M(NO)\}$ (mainly group 8 metals, particularly Ru, and $X =$ cyanides,⁶ amines,⁷ polypyridines,⁸ etc.) have been well characterized chemically and spectroscopically, including the corresponding aqua complexes $\{X_5M(H_2O)\}$. However, kinetic studies on the formation and dissociation reactions are generally absent, with the exception of very recent publications dealing with iron–nitrosyl complexes containing aqua,⁹ cyano,¹⁰ and different chelating ligands.¹¹

Transition metal–nitrosyl complexes span variable geometries, coordination numbers, and electronic properties, due to the differences in electronic configurations of the metal centers and covalent M–NO interactions.^{12,13} In the Enemark–Feltham electron-counting formalism,¹³ the complexes are described as $\{MNO\}^n$ (regardless of the spectator ligands), where n stands for the number of electrons associated with the metal d and π^*_{NO} orbitals. There are no assumptions on the actual degree of electron density on M and the NO group, thus avoiding extreme ways of describing

the nitrosyl oxidation states as NO^+ or NO^- , on the basis of the NO coordination mode (linear or bent, respectively), which sometimes leads to unusual metal oxidation state assignments. However, the delocalized nature of the $\{MNO\}$ fragment is frequently relaxed, by describing NO as a noninnocent ligand which can act as a diamagnetic, strongly π^* -accepting NO^+ , as the equally diamagnetic NO^- (iso-electronic with O_2), or as the paramagnetic, neutral NO. This limiting idealized behavior is used, for example, for the diamagnetic $\{MNO\}^6$ complexes with Werner-type spectator ligands, usually described as low-spin $M^{II}NO^+$ species, as is the case with NP. In the case of porphyrin $\{MNO\}^6$ systems, however, this description should hardly be generalized, because $M^{III}NO$ structures (or others) could also be inferred according to different spectroscopic measurements and their interpretation. Similar ambiguities have also been analyzed for the $\{MNO\}^7$ systems, which are most relevant to our presently reported work. In addition to the systems with total spin $S = 1/2$ (which are usually described as low-spin Fe^{II} with the bound NO-radical ($S = 1/2$)), the complexes with total spin $S = 3/2$ afford different possible bonding descriptions, with iron in the +I, +II, or +III oxidation states and NO in the +I, 0, or –I states, respectively.^{12–14}

The coordination chemistry of NO in aqueous solutions deals specifically with the radical species as the only possible reactant, because both NO^+ and NO^- (or its acid–base related “nitroxyl”, HNO) are transient species which react very rapidly before coordinating to the metal, generating nitrite or N_2O , respectively.^{1,2} Depending on the oxidation state of the counterpart aqua ion (usually II or III with group 8 metals), NO may be redox-active during the coordination process, involving some degree of electron transfer to the metal. For example, a recent study on the coordination of NO to $[Fe^{III}(CN)_5H_2O]^{2-}$ showed that prior reduction to $Fe(II)$ was needed with NO^+ formation, rapid conversion to nitrite, and final coordination and proton-assisted dehydration of the latter species, leading to NP as an unique product.¹⁰ In the present study, we address the coordination reaction of NO to the $[Fe^{II}(CN)_5H_2O]^{3-}$ ion. The kinetics and mechanisms for the coordination of a large series of L ligands to this aqua complex have been comprehensively studied.^{6,15} The present inclusion of NO appears to be quite attractive, given the scarce available kinetic information on its coordination ability. Great significance is assigned to such a biologically relevant issue as is the mechanism of controlled NO release from reduced NP.

Experimental Section

Materials. NO was purchased from Air Liquide and purified from higher nitrogen oxides by passing through an Ascarite II (Aldrich) column. Sodium nitroprusside dihydrate (Fluka), sodium dithionite (Merck), pyrazine (Aldrich), sodium cyanide (Merck), mercaptosuccinic acid (Aldrich), sodium nitrite (Merck), sodium perchlorate, and other chemicals used for the buffer systems were used without any further purification. $Na_3[Fe(CN)_5NH_3] \cdot 3H_2O$ was prepared and purified as described in the literature starting from

- (3) (a) Clarke, M. J.; Gaul, J. B. *Struct. Bonding (Berlin)* **1993**, 81, 147–181. (b) Butler, A. R.; Glidewell, C. *Chem. Soc. Rev.* **1987**, 16, 361–380.
- (4) (a) Ford, P. C.; Lorkovic, I. M. *Chem. Rev.* **2002**, 102, 993–1018. (b) Wolak, M.; van Eldik, R. *Coord. Chem. Rev.* **2002**, 230, 263–282.
- (5) Hoshino, M.; Laverman, L.; Ford, P. C. *Coord. Chem. Rev.* **1999**, 187, 75–102.
- (6) Baraldo, L. M.; Forlano, P.; Parise, A. R.; Slep, L. D.; Olabe, J. A. *Coord. Chem. Rev.* **2001**, 219–221, 881.
- (7) Tfouni, E.; Krieger, M.; McGarvey, B. R.; Franco, D. W. *Coord. Chem. Rev.* **2003**, 236, 57–69.
- (8) (a) Callahan, R. W.; Meyer, T. J. *Inorg. Chem.* **1977**, 16, 574–581. (b) Togano, T.; Kuroda, H.; Nagao, N.; Maekawa, Y.; Nishimura, H.; Howell, F. S.; Mukaida, M. *Inorg. Chim. Acta* **1992**, 196, 57–63.
- (9) Wanat, A.; Schnepfensieper, T.; Stochel, G.; van Eldik, R.; Bill, E.; Wiegardt, K. *Inorg. Chem.* **2002**, 41, 4–10.
- (10) Roncaroli, F.; Olabe, J. A.; van Eldik, R. *Inorg. Chem.* **2002**, 42, 5417–5425. In this reference, we argued that NO was acting as an outer-sphere electron transfer reagent toward the $[Fe^{III}(CN)_5H_2O]^{2-}$ ion. A colleague commented that our kinetic data could hardly support such a behavior, if the available redox potential data for the NO^+/NO couple and basic mechanistic requirements for the claimed outer-sphere path were considered. He suggested another possibility, implying an initial association of NO with coordinated cyanide in the precursor complex, leading to the stabilization of the produced NO^+ in the rate-determining step, and followed by the further chemistry as described by us. This could be accepted as an inner-sphere electron transfer pathway involving NO, without changing our main argument in favor of prior reduction of $Fe(III)$ in the absence of a change in the first coordination sphere, followed by the coordination of nitrite and conversion to NO^+ as found in NP.
- (11) (a) Schnepfensieper, T.; Finkler, S.; Czap, A.; van Eldik, R.; Heus, M.; Nieuwenhuizen, P.; Wreemann, C.; Abma, W. *Eur. J. Inorg. Chem.* **2001**, 491. (b) Schnepfensieper, T.; Wanat, A.; Stochel, G.; Goldstein, S.; Meyerstein, D.; van Eldik, R. *Eur. J. Inorg. Chem.* **2001**, 2317. (c) Schnepfensieper, T.; Wanat, A.; Stochel, G.; van Eldik, R. *Inorg. Chem.* **2002**, 41, 2565.
- (12) Westcott, B. L.; Enemark, J. L. In *Inorganic Electronic Structure and Spectroscopy, Volume II: Applications and Case Studies*; Solomon, E. I., Lever, A. B. P., Eds. Wiley: New York, 1999.
- (13) Enemark, J. H.; Feltham, R. D. *Coord. Chem. Rev.* **1974**, 13, 339–406.

- (14) Scheidt, W. R.; Ellison, M. K. *Acc. Chem. Res.* **1999**, 32, 359–359.
- (15) Macartney, D. H. *Rev. Inorg. Chem.* **1988**, 9, 101.

sodium nitroprusside.¹⁶ Its purity was checked by elemental analysis and by its reaction with pyrazine forming the $[\text{Fe}(\text{CN})_5\text{pz}]^{3-}$ ion.¹⁷

Methods. All the solutions were prepared using distilled and purified water (Milli-Q system) and deoxygenated by bubbling N_2 in Schlenk tubes. They were handled and mixed using gastight syringes. NO-saturated solutions were prepared by slowly bubbling NO through previously deoxygenated buffer solutions. The maximum concentration of NO in aqueous solution at room temperature is already known from our earlier work (1.8×10^{-3} M) and was checked with an ISO-NOP electrode interfaced to an ISO-NO Mark II nitric oxide sensor from World Precision Instruments, calibrated as described previously.^{11a} These solutions were diluted with buffer solutions to reach the final desired NO concentrations. Solutions of $[\text{Fe}(\text{CN})_5\text{L}]^{3-}$ ($\text{L} = \text{NH}_3, \text{H}_2\text{O}$) were prepared by dissolving the necessary amount of $\text{Na}_3[\text{Fe}(\text{CN})_5\text{NH}_3] \cdot 3\text{H}_2\text{O}$ in deoxygenated and thermostated (± 0.1 °C) buffer solutions. At $\text{pH} < 8$ and within 2–3 min, aqution of $[\text{Fe}(\text{CN})_5\text{NH}_3]^{3-}$ generates the $[\text{Fe}(\text{CN})_5\text{H}_2\text{O}]^{3-}$ complex.¹⁸ These solutions were generally used within 30 min after preparation. Solutions containing NP were stored in the dark and handled under diffuse light. Acetate buffers in the pH range 4–6, phosphate and Tris buffers in the pH range 6–8, and borate and CAPS (3-[cyclohexylamino]-1-propanesulfonic acid) buffers in the pH range 8–10 were used. The buffer concentrations were 0.01 M, unless otherwise stated. pH measurements were done with a Mettler Delta 340 pH meter.

UV-vis spectra were recorded on a Varian Cary 5G spectrophotometer. IR spectra of the products of the reaction of $[\text{Fe}(\text{CN})_5\text{H}_2\text{O}]^{3-}$ with NO were measured on an ATI Mattson Infinity FTIR 9495-120-12500 spectrometer, with a Perkin-Elmer liquid cell (CaF₂ windows, 0.2 mm spacer). Solutions were prepared by dissolving 10 mg of $\text{Na}_3[\text{Fe}(\text{CN})_5\text{NH}_3] \cdot 3\text{H}_2\text{O}$ in 100 mL of buffered solutions at pH 7 and 10. NO was bubbled through for 45 min, and the solutions were kept in the dark until the next day. Finally, N_2 was bubbled to eliminate excess of NO, and the volume was reduced to ca. 5 mL. During the concentration process, a small amount of a blue solid formed which was removed by filtration before measuring the IR spectrum. The mass spectrometric measurements were done using a GC-MS instrument, equipped with a Gerstel CIS3 injection module, a capillary GC Perkin-Elmer Autosystem XL, and an attached Quadrupole-MS Perkin-Elmer TurboMass. Databases were from commercial providers (NIST, NBS). The EPR spectra of 3×10^{-4} M solutions of $[\text{Fe}(\text{CN})_5\text{NO}]^{3-}$ (pH 10, prepared as described in a following paragraph) in frozen water (140 K) were recorded in the X-band of a Bruker ESP 300E spectrometer. The spectra were recorded at 9.47 GHz, 0.635 mW power, 100 kHz modulation frequency, and 9.434 G modulation amplitude.

Experiments in which aliquots of NO solutions were added to a buffered solution of $\text{Na}_3[\text{Fe}(\text{CN})_5\text{NH}_3] \cdot 3\text{H}_2\text{O}$ were performed in a 1 cm quartz cuvette directly attached to a round flask with sideway gas connections. In order to quantify the conversion into NP, an aliquot of the mother solution (ca. 10^{-4} M, at the desired pH) was mixed with the NO solution and then with a mercaptosuccinic acid solution, which led to the formation of the well characterized, stable red adduct between NP and mercaptosuccinic acid.¹⁹ The mixture was transferred to the cell under a flow of nitrogen, and the

absorbance at 526 nm was measured. In this way, the conversion into NP as a function of the amount of added NO could be studied. In order to determine the conversion into NP at different pH, NO was bubbled for 5 min through 40 mL of the 10^{-4} M $[\text{Fe}(\text{CN})_5\text{L}]^{3-}$ ($\text{L} = \text{NH}_3, \text{H}_2\text{O}$) solution, followed by mixing with the mercaptosuccinic acid solution.

Sodium dithionite was always used as a reductant for NP to generate the $[\text{Fe}(\text{CN})_5\text{NO}]^{3-}$ complex ($\lambda_{\text{max}} = 345$ and 440 nm; $\epsilon = 3500$ and $550 \text{ M}^{-1} \text{ cm}^{-1}$, respectively),²⁰ or the $[\text{Fe}(\text{CN})_4\text{NO}]^{2-}$ complex ($\lambda_{\text{max}} = 615, 430$, and 350 nm; $\epsilon = 380, 100$, and $300 \text{ M}^{-1} \text{ cm}^{-1}$, respectively).²⁰ In all cases, NP was about two times in excess to avoid multielectron reduction. The amount of dithionite was determined by titration of a solution of NP. After the addition of more than 1 equiv of dithionite, the band at 345 nm decreases, and a new band at 440 nm appears.

Kinetic experiments on the complex-formation reaction with NO at ambient pressure were performed on a Durrum (Dionex) stopped-flow instrument, equipped with a 2 cm optical path flow cell and coupled to an online data acquisition system. Equal volumes of both reactant solutions were mixed. Kinetic traces were analyzed by the Olis Kinfit program. At least five kinetic runs were performed at each condition, in many cases up to 12. In general, two or three independent experiments were performed under the same experimental conditions. The final observed rate constant, k_{obs} , was taken as the average of measurements that differed less than 15%. In the preliminary experiments, 10^{-4} M solutions of $[\text{Fe}(\text{CN})_5\text{H}_2\text{O}]^{3-}$ were mixed with an equal volume of 1.8×10^{-3} M solutions of NO. No electrolytes for ionic strength control were added. The temperature was kept at 25.4 °C. At $\text{pH} \leq 7$, the complex and NO solutions contained the same buffer (0.01 M), whereas at $\text{pH} \geq 8$ the complex solution was in 0.002 M acetic acid/acetate buffer at pH 5 and the NO solution was in 0.04 M boric acid/borate buffer at the final required pH value.

The influence of nitrite ions on the observed rate constant was studied by using a saturated NO solution with known amounts of NaNO_2 , viz. a final concentration of $(0.2\text{--}3.0) \times 10^{-2}$ M and pH 7.0. Some complementary experiments which involved changing the $[\text{Fe}(\text{CN})_5\text{H}_2\text{O}]^{3-}$ complex concentration or the buffer concentration were also done at pH 7.0.

The dependence of the complex-formation reaction on the concentration of NO, temperature and pressure was studied at pH 7.0 and $I = 0.1$ M (NaClO_4). For the NO concentration dependence study, the $[\text{Fe}(\text{CN})_5\text{H}_2\text{O}]^{3-}$ concentration was in the range $(1.0\text{--}5.0) \times 10^{-5}$ M, and the NO concentration was $(0.23\text{--}0.90) \times 10^{-3}$ M in order to have at least a 17-fold excess of NO at 25.4 ± 0.1 °C. A plot of k_{obs} versus $[\text{NO}]$ showed a linear dependence, and the slope enabled us to obtain the second-order rate constant, k_f . For the temperature dependence study, 5×10^{-5} M $[\text{Fe}(\text{CN})_5\text{H}_2\text{O}]^{3-}$ and 0.90×10^{-3} M NO were used, with the temperature varying in the range 15.0–44.6 °C. From the obtained k_{obs} values and the NO concentration, k_f was calculated for each temperature. Finally, an Eyring plot was used to determine the thermal activation parameters. For the pressure dependence study, a homemade high-pressure stopped-flow instrument was used, which has been described elsewhere.²¹ The 6×10^{-5} M $[\text{Fe}(\text{CN})_5\text{H}_2\text{O}]^{3-}$ and 9×10^{-4} M NO solutions were used at 25.6 ± 0.1 °C. The pressure was varied from 10 to 130 MPa. Time for temperature and pressure equilibration had to be allowed for after pressurizing the system.

(16) Kenney, D. J.; Flynn, T. P.; Gallini, J. B. *J. Inorg. Nucl. Chem.* **1961**, 20, 75.

(17) (a) Toma, E. H.; Malin, J. M. *Inorg. Chem.* **1973**, 12, 1039. (b) Toma, H. E.; Malin, J. M. *Inorg. Chem.* **1973**, 12, 2080.

(18) (a) Toma, H. E.; Malin, J. M. *Inorg. Chem.* **1974**, 13, 1772–1774. (b) Toma, H. E. *Inorg. Chim. Acta* **1975**, 15, 205–211.

(19) Szacilowski, K.; Stochel, G.; Stasicka, Z.; Kisch, H. *New J. Chem.* **1997**, 21, 893–902.

(20) Cheney, R. P.; Simic, M. G.; Hoffman, M. Z.; Taub, I. A.; Asmus, K. D. *Inorg. Chem.* **1977**, 16, 2187–2192.

(21) (a) van Eldik, R.; Palmer, D. A.; Schmidt, R.; Kelm, H. *Inorg. Chim. Acta* **1981**, 50, 131. (b) van Eldik, R.; Gaede, W.; Wieland, S.; Kraft, J.; Spitzer, M.; Palmer, D. A. *Rev. Sci. Instrum.* **1993**, 64, 1355.

This time increased with increasing pressure and varied between 20 and 60 min. Fortunately, the $[\text{Fe}(\text{CN})_5\text{H}_2\text{O}]^{3-}$ solution appeared to be more stable at higher pressures, where equilibration times were longer than under ambient conditions. When the kinetic traces became reproducible, they were averaged to obtain the k_{obs} values. A plot of $\ln k_{\text{obs}}$ versus P enabled the determination of the activation volume. A standard least-squares method (statistical function of Microsoft Excel) was employed to estimate the error limits of rate constants and activation parameters throughout this study.

For studies of the reverse dissociation reaction, ca. 3×10^{-4} M solutions of $[\text{Fe}(\text{CN})_5\text{NO}]^{3-}$ were prepared in two ways: either through reduction of NP with sodium dithionite, or through the reaction of a 1.5×10^{-3} M buffered solution of $[\text{Fe}(\text{CN})_5\text{H}_2\text{O}]^{3-}$ (pH 5, 0.01 M), with an equal volume of a 1.8×10^{-3} M solution of NO (pH 10.0, 0.1 M). In the first case, an aqueous solution of NP was mixed with a solution of ca. 0.5 equiv of sodium dithionite in 0.1 M buffer at pH 10.0. The final complex concentration of $[\text{Fe}(\text{CN})_5\text{NO}]^{3-}$ was calculated using the extinction coefficient reported in the literature (see a preceding description).²⁰ Pyrazine or sodium cyanide, as well as sodium perchlorate, was added to the final solutions where required. Spectral changes were recorded on a Varian Cary 5G spectrophotometer in the range 270–800 nm and were analyzed with the Specfit program.²² Preliminary experiments were performed at 25.0 and 45.1 °C.

The dependence of the dissociation rate constant, k_d , on temperature and pressure was studied at pH 10.2 (0.05 M buffer), $I = 0.1$ M (NaClO_4), $[\text{CN}^-] = 3 \times 10^{-2}$ M, and a complex concentration of ca. 3×10^{-4} M (obtained from the reaction between $[\text{Fe}(\text{CN})_5\text{H}_2\text{O}]^{3-}$ and NO as already described). Some experiments were carried out by varying the complex concentration between 1×10^{-4} and 3×10^{-3} M. The selected temperature range was 25.0–56.0 °C. The kinetic traces were analyzed as described, through the decrease in the 345 and 440 nm bands of $[\text{Fe}(\text{CN})_5\text{NO}]^{3-}$. Duplicate experiments were done at 25.0, 34.9, 50.5, and 45.1 °C.

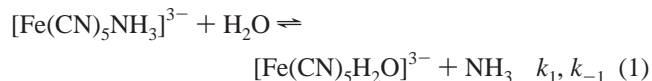
For the pressure dependence study, a 1.5 cm optical path length quartz pillbox cell was used. It was first filled with argon and then with the final $[\text{Fe}(\text{CN})_5\text{NO}]^{3-}$ solution. A high pressure optical cell unit described elsewhere²³ was used, and the spectral changes that accompany the back reaction were recorded at 347 nm on a Shimadzu UV-2101 PC spectrophotometer. Kinetic traces were analyzed by the Olis Kinfitt program. A single-exponential model was used, and kinetic traces could be fitted for approximately 5 half-lives of the reaction. The remaining conditions were the same as for the temperature dependence study. Some experiments were performed using 0.05 M CAPS buffer instead of 0.05 M borate buffer, without the addition of NaClO_4 . The temperature was 45.1 ± 0.1 °C. Two experiments under each condition were done in the range 5–150 MPa.

The reaction between $[\text{Fe}(\text{CN})_4\text{NO}]^{2-}$ and NO was studied by mixing buffered solutions of approximately 1.8×10^{-4} M $[\text{Fe}(\text{CN})_4\text{NO}]^{2-}$ with a saturated solution of NO at pH 5.0 or 7.0 and $I = 0.1$ M (NaClO_4). Kinetic traces were recorded at 615 nm.

Results and Discussion

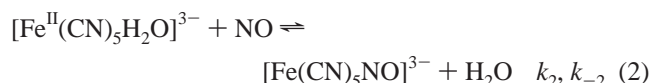
Since $\text{Na}_3[\text{Fe}(\text{CN})_5\text{NH}_3] \cdot 3\text{H}_2\text{O}$ is used as starting material, it is important to describe the appropriate conditions for the generation and handling of the reactants. This complex is

known to undergo a rapid aquation reaction,^{18a} according to reaction 1:



Data reported for reaction 1 are the following: $k_1 = 1.75 \times 10^{-2} \text{ s}^{-1}$, $k_{-1} = 452 \text{ M}^{-1} \text{ s}^{-1}$, and $K_1 = 3.9 \times 10^{-5} \text{ M}$ at 25 °C.^{18a,24,25} We, therefore, expect a rapid (ca. 40 s half-life), almost complete aquation in a few minutes after dissolution of the ammine complex, provided the work is carried out in the pH range 4–8, where NH_3 is trapped as NH_4^+ and cannot react as a nucleophile (note that the $\text{p}K_a$ for NH_4^+ is 9.24).²⁶ The reactant and product complexes absorb at 396 nm ($\epsilon = 450 \text{ M}^{-1} \text{ cm}^{-1}$)²⁴ and 440 nm ($\epsilon = 640 \text{ M}^{-1} \text{ cm}^{-1}$),^{18b} respectively, allowing for an easy discrimination between these species. Even up to pH 10, reaction 1 is expected to be driven almost completely to the right for sufficiently diluted solutions of the complex. In this way, at the $(1-5) \times 10^{-5} \text{ M}$ concentration level, the cyano-bridged dimerization reaction of the aqua complex can be prevented.²⁷ No complications related to the protonation of coordinated cyanide (the $\text{p}K_a$ values for bound HNC ligands are between 0 and 3)^{17,28} or to the deprotonation of $[\text{Fe}(\text{CN})_5\text{H}_2\text{O}]^{3-}$ ^{27b} are expected to occur in the selected pH range 4–10. Finally, the $[\text{Fe}(\text{CN})_5\text{H}_2\text{O}]^{3-}$ ion is known to decompose thermally by release of cyanide ($k = \text{ca. } 10^{-4} \text{ s}^{-1}$ at 25 °C);²⁹ this unavoidable process can be controlled by using freshly prepared solutions in all experiments.

The reaction under study can be described by eq 2:



The product of reaction 2 has been previously obtained upon reduction of NP with different chemical reducing agents (viz. dithionite, tetrahydroborate, and sodium in liquid ammonia),^{30–32} as well as electrochemically³³ and by pulse radiolysis techniques.²⁰ It has been isolated as a sodium salt³² (no crystal structure is available) and has been characterized by different spectroscopic techniques (UV–vis,²⁰ IR,³² and EPR³⁰). Recent DFT calculations on $[\text{Fe}(\text{CN})_5\text{NO}]^{3-}$, together with the Ru and Os analogues, have confirmed the original EPR assignment³⁰ and have supported the electronic structure

(22) (a) Binstead, R. A.; Zuberbühler, A. D. *Specfit*; Spectrum Software Associates: Chapel Hill, NC, 1993–1999. (b) Zuberbühler, A. D. *Anal. Chem.* **1990**, *62*, 2220.

(23) Spitzer, M.; Gärtig, F.; van Eldik, R. *Rev. Sci. Instrum.* **1988**, *59*, 2092.

(24) Toma, H. E.; Batista, A. A.; Gray, H. B. *J. Am. Chem. Soc.* **1982**, *104*, 7509–7515.

(25) Maciejowska, I.; van Eldik, R.; Stochel, G.; Stasicka, Z. *Inorg. Chem.* **1997**, *36*, 5409–5412.

(26) Fasman, G. D. *Handbook of Biochemistry and Molecular Biology, Physical and Chemical Data*; CRC Press: Cleveland, OH, 1976; Vol. 1.

(27) (a) Davies, G.; Garafalo, A. R. *Inorg. Chem.* **1976**, *15*, 1101–1106. (b) Davies, G.; Garafalo, A. R. *Inorg. Chem.* **1980**, *19*, 3543–3544.

(28) Malin, J. M.; Koch, R. C. *Inorg. Chem.* **1978**, *17*, 752–754.

(29) Zerga, H. O.; Olabe, J. A. *Inorg. Chem.* **1983**, *22*, 4156–4158.

(30) van Voorst, J. D. W.; Hemmerich, P. *J. Chem Phys.* **1966**, *45*, 3914–3918.

(31) Bertolino, J. R.; Della Védova, C. O.; Sala, O. *Polyhedron*, **1989**, *8*, 361–365.

(32) Nast, R.; Schmidt, J. *Angew. Chem., Int. Ed. Engl.* **1969**, *8*, 383.

(33) Masek, J.; Maslova, E. *Collect. Czech. Chem. Commun.* **1974**, *39*, 2141–2160.

as corresponding to a $\{\text{FeNO}\}^7$ system, with an angular FeNO bond and a spin distribution at the singly occupied molecular orbital (SOMO) mainly localized at the NO ligand (ca. 62%), with around 29% at iron.³⁴ On this basis, the electronic structure of $[\text{Fe}(\text{CN})_5\text{NO}]^{3-}$ can be described as a low-spin $\{\text{Fe}^{\text{II}}\text{NO}\}$ species, also supported by the NO stretching frequency at 1608 cm^{-1} , which is quite down-shifted compared to the one in NP, viz. 1940 cm^{-1} , formally described as $\{\text{Fe}^{\text{II}}\text{NO}^+\}$.³⁵ It is in agreement with a reduction mainly localized at the NO ligand, which decreases significantly the N–O bond order.

The $[\text{Fe}(\text{CN})_5\text{NO}]^{3-}$ ion decomposes by releasing cyanide according to reaction 3:



Equilibrium and kinetic parameters have been determined and are $k_3 = 2.7 \times 10^2\text{ s}^{-1}$, $k_{-3} = 4 \times 10^6\text{ M}^{-1}\text{ s}^{-1}$, and $K_3 = 6.8 \times 10^{-5}\text{ M}$.²⁰ These values indicate that variable amounts of the penta- and the tetra-cyano species will be present in aqueous solution depending on the pH. A dominant contribution of $[\text{Fe}(\text{CN})_5\text{NO}]^{3-}$ appears in the mixtures prepared at pH values greater than 8, as demonstrated by the UV–vis spectra. However, some $[\text{Fe}(\text{CN})_4\text{NO}]^{2-}$ ion is always present, and its relative amount increases on decreasing the pH since the proton-assisted elimination of cyanide displaces equilibrium to the right. Reaction 3 also predicts that, in the presence of added cyanide, the solutions obtained by reduction of NP will contain predominantly the pentacyano complex (see a following paragraph for studies on the dissociation of NO).

The Complex-Formation Reaction (Forward Step in Reaction 2). Figure 1 describes preliminary experiments in which spectra were obtained upon successive addition of 1 mL aliquots of an NO-saturated solution to an aqueous solution of $\text{Na}_3[\text{Fe}(\text{CN})_5\text{NH}_3] \cdot 3\text{H}_2\text{O}$ at pH 10. Approximately 5 min elapsed between the addition of subsequent aliquots, and the complete experiment was performed within 30 min. The intensity of the 440 nm band of $[\text{Fe}(\text{CN})_5\text{H}_2\text{O}]^{3-}$ (formed via fast aquation in reaction 1)^{18a} decreases upon addition of NO, while new bands at 347 and 620 nm appear. Although 0.95 equiv of NO was consumed, the band at 347 nm reached only 20% of the intensity expected for a 100% conversion of $[\text{Fe}(\text{CN})_5\text{H}_2\text{O}]^{3-}$ into $[\text{Fe}(\text{CN})_5\text{NO}]^{3-}$ (reaction 2). Upon further addition of NO, all of the already-mentioned bands disappeared, and only a shoulder at ca. 330–350 nm remained. NO (1.9 equiv) was consumed in the total process. An IR spectrum of the final solution treated with an excess of NO showed bands corresponding to the formation of NP at 1936 and 2142 cm^{-1} .³⁵ The yield of NP was ca. 100% in reference to the initial aqua complex concentration. The product solution showed no reaction with pyrazine,¹⁷ consistent with the extremely inert nature of the NO^+ ligand toward substitution in NP. The inset of Figure 1 shows kinetic

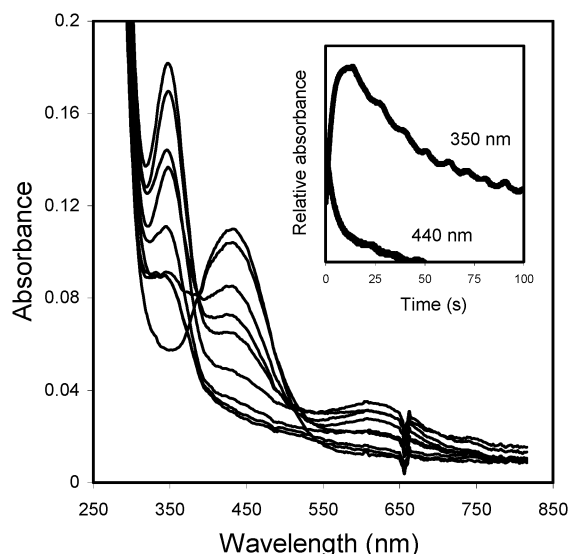


Figure 1. Spectral changes corresponding to successive addition of 1 mL aliquots of NO-saturated solution ($1.8 \times 10^{-3}\text{ M}$) to 40 mL of a $3 \times 10^{-4}\text{ M}$ $[\text{Fe}(\text{CN})_5\text{NH}_3]^{3-}$ solution (pH = 10.0; 0.01 M borate buffer). The continuous decrease of the 440 nm band parallels the initial increase and subsequent decrease of the bands at 347 and 620 nm. The final pH was unchanged. Inset: Kinetic traces at 440 and 350 nm upon mixing equal volumes of an NO-saturated solution, (pH 10.0; 40 mM borate buffer) and a $5 \times 10^{-5}\text{ M}$ $[\text{Fe}(\text{CN})_5\text{H}_2\text{O}]^{3-}$ solution (pH 5; 0.02 M acetate buffer).

traces recorded at 440 and 350 nm for a related experiment performed under excess of NO. It can be seen that a fast process occurs in the first few seconds followed by a slow decay of the bands. The kinetic traces are consistent with reaction 2 and show that the rapid spectral change corresponds to the formation of the nitrosyl complex. The subsequent decay at 350 nm observed over longer times is consistent with the low yields of the nitrosyl complex already described and indicates that the $[\text{Fe}(\text{CN})_5\text{NO}]^{3-}$ complex produced initially is not stable under the selected reaction conditions.³⁶

At pH 7, Figure 2 (obtained under similar conditions as Figure 1) shows a similar but not identical picture. The band at 440 nm also decays continuously upon addition of NO, but no formation of an intermediate at ca. 350 nm is observed as was observed in Figure 1. The final product absorbs at ca. 320 nm accompanied by an increase in the baseline around 550–800 nm with the clear appearance of two isosbestic points. These spectral features were also observed for similar experiments at pH 4–8. In the overall process,

(36) We found that both $[\text{Fe}(\text{CN})_5\text{NO}]^{3-}$ and $[\text{Fe}(\text{CN})_4\text{NO}]^{2-}$, generated as predominant species in solution at pH 10 and 6–7, respectively, reacted with excess NO, showing a rapid decrease in their characteristic absorption bands. This is supported by the fast cyanide release from $[\text{Fe}(\text{CN})_5\text{NO}]^{3-}$ (see text) and also by the fast reaction of $[\text{Fe}(\text{CN})_4\text{NO}]^{2-}$ with NO (k_{obs} , 58 s^{-1} , our measurements, see Experimental Section), consistent with the reported fast decomposition of $[\text{Fe}(\text{CN})_5\text{NO}]^{3-}$ at pH 7. However, when cyanide was added to the solution of $[\text{Fe}(\text{CN})_5\text{NO}]^{3-}$ at pH 10, no decomposition was observed. Given equilibrium 3, this indicates that NO must react with $[\text{Fe}(\text{CN})_4\text{NO}]^{2-}$, but not with $[\text{Fe}(\text{CN})_5\text{NO}]^{3-}$. The mode of decomposition is presently under study. We report in the present study some preliminary results that show the final formation of NP, with an increase in conversion at increasing pH, together with the apparent formation of $[\text{Fe}(\text{CN})_6]^{4-}$ under some conditions. If a disproportionation of bound NO is operative (cf. ref 32), we are still unable to define the product of NO reduction.

(34) Wanner, M.; Scheiring, T.; Kaim, W.; Slep, L. D.; Baraldo, L. M.; Olabe, J. A.; Zalis, S.; Baerends, E. J. *Inorg. Chem.* **2001**, *40*, 5704–5707.

(35) Paliani, G.; Poletti, A.; Santucci, A. *J. Mol. Struct.* **1971**, *8*, 63–74.

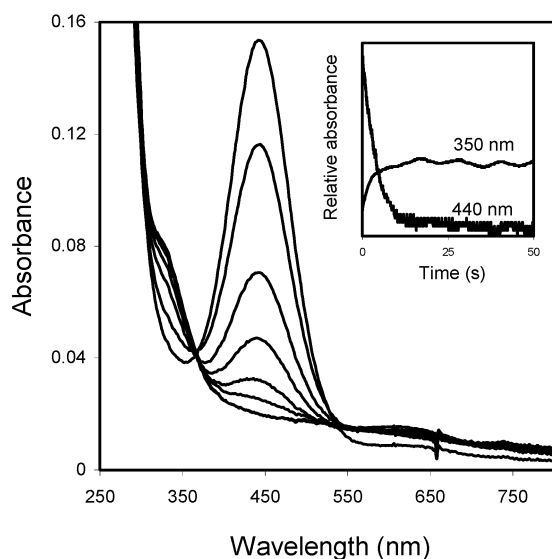


Figure 2. Spectral changes corresponding to successive additions of 1 mL aliquots of NO-saturated solution, 1.8×10^{-3} M, to 40 mL of a 2.8×10^{-4} M $[\text{Fe}(\text{CN})_5\text{H}_2\text{O}]^{3-}$ solution (pH = 7.0, 0.01 M Tris buffer). The final pH was unchanged. Inset: Kinetic traces at 440 and 350 nm upon mixing equal volumes of NO-saturated and 5×10^{-5} M $[\text{Fe}(\text{CN})_5\text{H}_2\text{O}]^{3-}$ solutions (same buffer system).

0.95 equiv of NO were consumed. The IR spectrum of the reaction product in the presence of an excess of NO also showed the characteristic bands of NP, together with an additional band at 2036 cm^{-1} that can be assigned to the formation of $[\text{Fe}(\text{CN})_6]^{4-}$,^{4–37} consistent with the product shoulder at 320 nm .³⁸ The corresponding inset in Figure 2 shows a single kinetic process. The traces at 440 and 350 nm fit a single exponential function for at least three half-lives, usually five half-lives, of the reaction.³⁹ The observed rate constants, k_{obs} 's, obtained from kinetic traces at both wavelengths were essentially the same. Note that the half-lives for the absorbance decrease at 440 nm are practically the same for the experiments at pH 10 and 7 (insets in Figures 1 and 2, respectively), although no intermediates are detected in the latter case. This confirms that the decrease at 440 nm effectively corresponds to the forward reaction in eq 2, with the product decomposing faster at lower pH. Table 1 summarizes the data obtained for the preliminary experiments. No pH dependence was observed for k_{obs} in the range 4–7, with an average value of 0.23 s^{-1} at $25\text{ }^\circ\text{C}$. Even the results in the pH range 8–10, using a different mixing procedure in order to avoid the perturbations caused by aquation of $[\text{Fe}(\text{CN})_5\text{NH}_3]^{3-}$ (see Experimental Section), revealed similar values for the rate constants.

(37) Jones, L. H. *Inorg. Chem.* **1963**, 2, 777–780.

(38) Alexander, J. J.; Gray, H. B. *J. Am. Chem. Soc.* **1968**, 90, 4260–4271.

(39) The trace at 350 nm appears noisy in the stabilized region, because the measurement was not performed at the appropriate wavelength, namely 320 nm , where the final product absorbs. At that time, we had in mind that an intermediate absorbing at 345 nm could be present. This is evidently not the case, as shown in Figure 2 in the main series of recorded spectra. The overall kinetic trace in the inset, and most importantly the rising part, is significant and shows the same kinetic performance as observed for the one at 440 nm . This is evidence for the initial formation and very fast decay of $[\text{Fe}(\text{CN})_5\text{NO}]^{3-}$ at pH 7 (see text and previous comment in ref 36).

Table 1. Preliminary Results for Complex-Formation Reaction 2^a

$[\text{Fe}(\text{CN})_5\text{H}_2\text{O}]^{3-}$ (mM)	pH	$[\text{NO}_2^-]$ (mM)	k_{obs}^b (s^{-1})
0.05	4.0		0.22
0.05	5.0		0.24
0.05	6.0		0.22
0.05	7.0		0.23 (0.23)
0.05	8.0		0.24 (0.22)
0.05	9.0		0.24 (0.21)
0.05	10.0		0.22 (0.24)
0.05	7.0	2.0	0.22
0.05	7.0	5.9	0.23
0.05	7.0	9.4	0.35
0.05	7.0	15.6	0.40
0.05	7.0	19.2	0.41
0.05	7.0	30.1	0.54
0.01	7.0		0.26
0.02	7.0		0.22
0.06	7.0		0.24
0.10	7.0		0.35

^a $T = 25.4\text{ }^\circ\text{C}$; $[\text{NO}] = 0.9\text{ mM}$. ^b Values in parentheses were calculated from the absorbance increase at 350 nm , the remaining from the absorbance decrease at 440 nm .

The possible influence of unavoidable nitrite impurities always present in aqueous solutions of NO (which may reach a level of around 10^{-4} M) inspired a series of experiments on the dependence of k_{obs} on the concentration of nitrite in the test solutions (see Table 1). Increasing amounts of nitrite, up to 30-fold as compared to $[\text{NO}]$, were used, and it was found that no significant effect was observed up to a concentration of $6 \times 10^{-3}\text{ M}$, with some increase in the observed rate constant for higher concentrations. The latter results are understandable, since both nitrite²⁷ and NO effectively bind to $[\text{Fe}(\text{CN})_5\text{H}_2\text{O}]^{3-}$ in a competitive way, and then the measured rate constant will be the sum of both contributions. Since the second-order formation rate constant for the coordination of nitrite is approximately an order of magnitude smaller than for NO,²⁷ the results for k_{obs} in Table 1 can be understood. The error introduced by nitrite is at the 1% level for NO solutions that contain the usual nitrite impurity. This error is by far overcome by the normal experimental error limits of ca. 10% in these measurements.

The percentage conversion of $[\text{Fe}(\text{CN})_5\text{H}_2\text{O}]^{3-}$ into NP in the presence of an excess of NO was studied as a function of pH: % (pH) = 35–45 (3–5.5); 60 (7); 75 (8); 95–100 (8.5–10). This suggests that, at the more acidic pH, the free cyanide generated through reaction 3 becomes protonated and is unable to recombine with the rapidly formed tetracyano species in order to form NP.³⁶

Figure 3 shows the dependence of k_{obs} (s^{-1}) on the concentration of NO, from which the second-order rate constant, $k_2 = 250 \pm 10\text{ M}^{-1}\text{ s}^{-1}$ at $25.4\text{ }^\circ\text{C}$, $I = 0.1\text{ M}$, and pH 7.0, can be calculated from the slope of the line. As shown in Table 3, this value is in close agreement with earlier data for the rate constants obtained for the coordination of neutral ligands to $[\text{Fe}(\text{CN})_5\text{H}_2\text{O}]^{3-}$, which cover a range from 200 to $450\text{ M}^{-1}\text{ s}^{-1}$. In contrast, positively and negatively charged ligands usually show larger or smaller rate constants, respectively.¹⁵ The results in Figure 3, furthermore, indicate that the rate constant for the reverse reaction, k_{-2} , represented

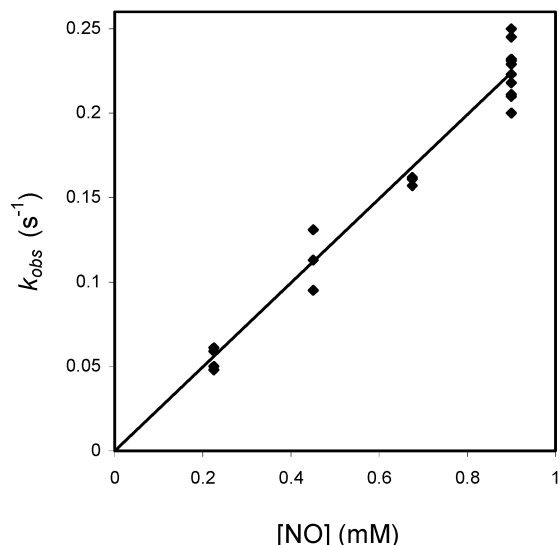


Figure 3. Dependence of k_{obs} on the concentration of NO for the complex-formation reaction: $T = 25.4 \pm 0.1$ °C, pH = 7.0 (0.01 M tris), $I = 0.1$ M (NaClO_4), $[\text{Fe}(\text{CN})_5\text{H}_2\text{O}^{3-}] = (1-5) \times 10^{-5}$ M, $[\text{NO}] = (0.23-0.90) \times 10^{-3}$ M. For a given $[\text{NO}]$, distinctive values of k_{obs} represent the spread in the measurements, at a constant complex concentration. From the slope, $k_2 = 250 \pm 10 \text{ M}^{-1} \text{ s}^{-1}$.

Table 2. Kinetic Results for Complex-Formation Reaction 2 at pH = 7.0 and $I = 0.1 \text{ M}^a$

$[\text{Fe}(\text{CN})_5\text{H}_2\text{O}^{3-}]$ (mM)	$[\text{NO}]$ (mM)	temp (°C)	pressure (MPa)	k_{obs} (s^{-1})
0.05	0.90	25.4	0.1	0.23 ± 0.01
0.04	0.68	25.4	0.1	0.16 ± 0.01
0.02	0.45	25.4	0.1	0.11 ± 0.01
0.01	0.23	25.4	0.1	0.054 ± 0.005
1.1	0.1	25.4	0.1	0.29 ± 0.02
0.05	0.90	29.9	0.1	0.30 ± 0.01
0.05	0.90	35.3	0.1	0.54 ± 0.02
0.05	0.90	40.1	0.1	0.82 ± 0.03
0.05	0.90	44.6	0.1	1.29 ± 0.01
0.05	0.90	20.9	0.1	0.13 ± 0.01
0.05	0.90	15.0	0.1	0.077 ± 0.008
0.06	0.90	25.6	10	0.237 ± 0.004
0.06	0.90	25.6	50	0.182 ± 0.003
0.06	0.90	25.6	90	0.135 ± 0.003
0.06	0.90	25.6	130	0.103 ± 0.001

^a k_2 (25.4 °C) = $250 \pm 10 \text{ M}^{-1} \text{ s}^{-1}$, $\Delta H_2^\ddagger = 70 \pm 1 \text{ kJ mol}^{-1}$, $\Delta S_2^\ddagger = +34 \pm 4 \text{ J K}^{-1} \text{ mol}^{-1}$, $\Delta V_2^\ddagger = +17.4 \pm 0.3 \text{ cm}^3 \text{ mol}^{-1}$.

by the intercept is indeed very small and cannot be obtained in this way.

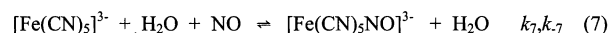
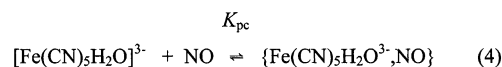
Table 2 summarizes the kinetic data obtained for the complex-formation reaction at different temperatures and pressures, from which the activation parameters were calculated (see Figures S1 and S2, Supporting Information). Table 3 shows that the value of the activation enthalpy, $70 \pm 1 \text{ kJ mol}^{-1}$, is very similar to values obtained for a wide range of neutral ligands. In general, there is little variation in this parameter with values around $60-80 \text{ kJ mol}^{-1}$. The positive activation entropy, viz. $+34 \pm 4 \text{ J K}^{-1} \text{ mol}^{-1}$, is also consistent with values reported for other entering ligands, although in this case the variation is larger. Finally, the activation volume for the reaction with NO was found to be $+17.4 \pm 0.3 \text{ cm}^3 \text{ mol}^{-1}$. Some examples from earlier reports for the coordination of other neutral and negatively charged ligands to $[\text{Fe}(\text{CN})_5\text{H}_2\text{O}]^{3-}$ are consistent with that found

Table 3. Complex-Formation Rate Constants and Activation Parameters for Different $[\text{Fe}(\text{CN})_5\text{L}]^{n-}$ Complexes^a

L	k_f ($\text{M}^{-1} \text{ s}^{-1}$)	ΔH_f^\ddagger (kJ mol^{-1})	ΔS_f^\ddagger ($\text{J K}^{-1} \text{ mol}^{-1}$)	ΔV_f^\ddagger ($\text{cm}^3 \text{ mol}^{-1}$)	ref
$N\text{-Mepz}^{+b,c}$	550 ^b	70.3	+42		17
	2350 ^c				15
CO^c	310	63	+15		40
NO^c	250	70	+34	+17.4	this work
dmsO^b	240	64.4	+16.7		41
pz^d	380	64.4	+20.9		17
his^c	315	64.4	+21	+17.0	42,43
py^d	365	67.4	+29.3		17
NH_3^c	365	62	+10	+14.4	24,25
	452	78	+67		
Im^c	242	63.5	+12.5	+15.5	42,43
CN^{-b}	30	76.9	+42	+13.5	44

^a For the following reaction: $[\text{Fe}(\text{CN})_5\text{H}_2\text{O}]^{3-} + \text{L} \rightarrow [\text{Fe}(\text{CN})_5\text{L}]^{n-} + \text{H}_2\text{O}$, $T = 25.0$ °C, except for $\text{L} = \text{NO}$, $T = 25.4$ °C. ^b $I = 1 \text{ M}$. ^c $I = 0.1 \text{ M}$. ^d $I = 0.5 \text{ M}$.

Scheme 1



for NO (see Table 3). The consistent rate constants found for the complex-formation reactions with different ligands of similar charge, as well as the almost constant, positive values for the activation entropy and activation volume, suggest the operation of a dissociative mechanism.⁴⁵ Two possible pathways can be considered, as outlined in Scheme 1 for the reaction with NO.

The first pathway is presented by the route described by reactions 4 and 6, which involves a dissociative interchange (I_d) mechanism.⁴⁵ Reaction 4 implies the rapid formation of a precursor complex, followed by the slow ligand interchange step (6) between the first and second coordination spheres of the precursor complex. In this case, the derived rate law is given by $k_{\text{obs}} = k_6 K_{\text{pc}} [\text{NO}] / (1 + K_{\text{pc}} [\text{NO}]) + k_{-6}$, which simplifies to $k_{\text{obs}} = k_6 K_{\text{pc}} [\text{NO}]$ under our reaction conditions (see Figure 3).¹⁵ An alternative pathway is given by reactions 5 and 7 and represents a limiting dissociative (D) mechanism,⁴⁵ in which the slow release of water in reaction 5 to form a pentacoordinate intermediate is followed by the rapid coordination of NO. In this case, the rate law has a similar form: $k_{\text{obs}} = (k_5 k_7 [\text{NO}] + k_{-7}) / (k_7 [\text{NO}] + k_{-5} [\text{H}_2\text{O}])$, which simplifies to $k_{\text{obs}} = k_5 k_7 [\text{NO}] / k_{-5} [\text{H}_2\text{O}]$ under our conditions. A variation on the I_d mechanism has been proposed, viz. the D_{pc} mechanism, in which the rate-limiting loss of the

- (40) Toma, H. E.; Moroi, N. M.; Iha, N. Y. M. *An. Acad. Bras. Cienc.* **1982**, *54*, 315–323.
- (41) Toma, H. E.; Malin, J. M.; Giesbrecht, E. *Inorg. Chem.* **1973**, *12*, 2084.
- (42) Toma, H. E.; Martins, J. M.; Giesbrecht, E. *J. Chem. Soc., Dalton Trans.* **1981**, 1610–1617.
- (43) Stochel, G.; Chatlas, J.; Martínez, P.; van Eldik, R. *Inorg. Chem.* **1992**, *31*, 5480–5483.
- (44) Finston, M. I.; Drickamer, H. G. *J. Phys. Chem.* **1981**, *104*, 7509–7515.
- (45) Langford, C. H.; Gray, H. B. *Ligand Substitution Processes*; W. A. Benjamin, Inc.: Reading, MA, 1965.

aqua ligand occurs within the precursor complex.¹⁵ It can be seen that the proposed mechanisms agree with the second-order behavior found in Figure 3. The slight but significant dependence of k_2 on the charge of the entering ligand (see Table 3) is accounted for in the I_d and D_{pc} mechanisms by the different values of K_{pc} , which must increase with the positive charge on the entering ligand. On the other hand, the D mechanism can account for this fact through the electrostatic effects that influence the value of k_7 .⁴³ Other arguments have been presented in favor of the limiting D pathway; one of them is based on the principle of microscopic reversibility, since strong evidence exists for the operation of a limiting D mechanism for the reverse dissociation process. Furthermore, particular emphasis has been placed on the fact that the volumes of activation cover a range from +14 to +18 cm³ mol⁻¹ for a wide range of neutral and negatively charged entering ligands (Table 3).⁴³ The range of values is rather consistent with the limiting value calculated for the dissociation of a water molecule from an octahedral metal center, viz. +13.1 cm³ mol⁻¹.⁴⁶ The presently reported value for complex-formation with NO agrees with this proposal. For a series of high-spin Fe^{II}(L) complexes, with L = aqua and diverse polycarboxylate ligands, the reversible binding of NO afforded small values for the activation volumes, supporting an I_d mechanism. A comparison within the {FeNO}⁷ systems must be done with caution, because in the already-mentioned complexes the electronic structure is quite different from that in [Fe(CN)₅NO]³⁻.^{4,9,11} Similarly, high formation rates and small activation volumes have been found for the formation of NO complexes with some ferroporphyrins.⁴

The Ligand Dissociation Reaction (Reverse Step in Reaction 2). The [Fe(CN)₅NO]³⁻ complex can be generated in solution via the reaction of [Fe(CN)₅H₂O]³⁻ with NO at pH 10, or upon reduction of NP with dithionite. The EPR spectra recorded for frozen solutions of [Fe(CN)₅NO]³⁻ were found to be the same as previously reported by van Voorst and Hemmerich (see Figure S3, Supporting Information).³⁰ This result, together with the characteristic UV-vis spectral signatures, confirms the identity of the product in reaction 2. Spectral changes that correspond to the decay of [Fe(CN)₅NO]³⁻ at pH 10 in the absence of any other potential ligand could not be fitted to a single-exponential function. This was the case for [Fe(CN)₅NO]³⁻ generated by any of the procedures mentioned already. Upon addition of pyrazine to the system, a decrease of the band at 347 nm and an increase in the absorbance at ca. 450 nm were observed, which were assigned to the formation of the [Fe(CN)₅pz]³⁻ complex ($\lambda_{max} = 452$ nm, $\epsilon = 5000$ M⁻¹ cm⁻¹).¹⁷ However, first-order kinetics were still not observed. In addition, there was also a small but appreciable absorbance at 615 nm due to the presence of [Fe(CN)₄NO]²⁻, which also decayed in the same process. Finally, Figure 4 shows the spectral changes observed after addition of sodium cyanide to the [Fe(CN)₅NO]³⁻ complex solution. Now the kinetic traces at 347 and 440 nm (see inset in Figure 4) obeyed a first-order

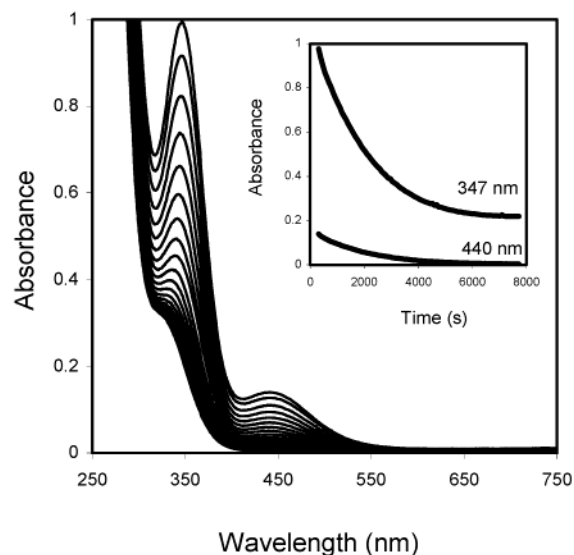
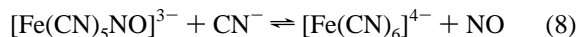


Figure 4. Spectral changes recorded during the dissociation of NO from the [Fe(CN)₅NO]³⁻ complex in the presence of free cyanide: [Fe(CN)₅NO]³⁻ = 3×10^{-4} M, pH 10.2 (0.05 M borate buffer), $I = 0.1$ M (NaClO₄), [CN⁻] = 0.03 M, $T = 50.4$ °C, cycle time 312 s. Inset: Kinetic traces at 440 and 347 nm, $k_{obs} = 5.14 \times 10^{-4}$ s⁻¹.

behavior. Only a shoulder at ca. 320 nm remained, which can be assigned to the presence of [Fe(CN)₆]⁴⁻ (see preceding description).³⁸ No bands in the range 500–800 nm were detected.

Figure 4 shows that the NO ligand is substituted by cyanide in the overall reaction 8.



As a result of cyanide addition, reaction 8 now appears as a clean substitution process, free of the presence of the initial [Fe(CN)₄NO]²⁻ complex (compare reaction 3). NO was detected qualitatively as a product in the thermal decomposition of a 3 mM [Fe(CN)₅NO]³⁻ solution using electrochemical and mass spectrometric detection techniques.

The data for the dissociation reaction at different temperatures and pressures are summarized in Table 4.⁴⁷ The average observed rate constant (k_{-2}) was found to be $(1.58 \pm 0.06) \times 10^{-5}$ s⁻¹ at 25.0 °C, $I = 0.1$ M, and pH 10.2. Table 5 summarizes dissociation rate constants and activation parameters for the release of different ligands L from pentacyanoferrate(II) fragments.

The activation parameters, ΔH_{-2}^\ddagger , ΔS_{-2}^\ddagger , and ΔV_{-2}^\ddagger , were found to be 106.4 ± 0.8 kJ mol⁻¹, $+20 \pm 2$ J K⁻¹ mol⁻¹, and $+7.1 \pm 0.2$ cm³ mol⁻¹, respectively. The temperature and pressure dependence plots are shown in Figures S4 and S5 (Supporting Information), respectively. As seen from the summary of data in Table 5, the activation enthalpies and entropies are consistent with those reported for the release of other ligands from the pentacyanoferrate(II) fragment.^{48–53}

(47) Although not included in Table 4, some experiments were performed by changing the initial complex concentration, by going up 10-fold and down 3-fold with respect to the data in Table 4. This was done in search for any possible second-order pathway allowing for alternative decomposition modes of [Fe(CN)₅NO]³⁻, viz., a bimolecular dismutation process. No significant difference in the k_{obs} values was found.

(46) Swaddle, T. W. *Inorg. Chem.* **1983**, 22, 2663–2665.

Table 4. Kinetic Results for the Dissociation of NO from $[\text{Fe}(\text{CN})_5\text{NO}]^{3-}$ ^a

temp (°C)	pressure (MPa)	$k_{\text{obs}} \times 10^4$ (s ⁻¹)
25.0	0.1	0.158 ± 0.006
30.3	0.1	0.34 ± 0.01
34.9	0.1	0.68 ± 0.01
38.3	0.1	1.10 ± 0.05
45.1	0.1	2.6 ± 0.3
50.5	0.1	5.3 ± 0.2
56.0	0.1	9.8 ± 0.3
45.1	5	2.55 ± 0.01
45.1	50	2.24 ± 0.01
45.1	100	1.99 ± 0.01
45.1	150	1.84 ± 0.03
45.1	150	1.70 ± 0.01^b

^a pH 10.2; $I = 0.1$ M; $[\text{Fe}(\text{CN})_5\text{NO}^{3-}] = \text{ca. } 3 \times 10^{-4}$ M; $[\text{CN}^-] = 0.030$ M. k_{-2} (25.0 °C) = $(1.58 \pm 0.06) \times 10^{-5} \text{ s}^{-1}$, $\Delta H_{-2}^\ddagger = 106.4 \pm 0.8$ kJ mol⁻¹, $\Delta S_{-2}^\ddagger = +20 \pm 2 \text{ J K}^{-1} \text{ mol}^{-1}$, $\Delta V_{-2}^\ddagger = +7.1 \pm 0.2 \text{ cm}^3 \text{ mol}^{-1}$.
^b CAPS buffer was used instead of boric acid/borate buffer. This value was used instead of the previous one in order to prevent errors associated with the dependence of the $\text{p}K_a$ value of the boric acid/borate buffer upon pressure.

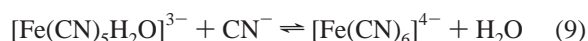
Table 5. Dissociation Rate Constants and Activation Parameters for Different $[\text{Fe}(\text{CN})_5\text{L}]^{n-}$ Complexes^a

ligand	k_d (s ⁻¹)	ΔH_d^\ddagger (kJ mol ⁻¹)	ΔS_d^\ddagger (J K ⁻¹ mol ⁻¹)	ΔV_d^\ddagger (cm ³ mol ⁻¹)	ref
CO ^{bc}	$<10^{-8}$				40
CN ^{-cd}	$\text{ca. } 4 \times 10^{-7}$				48
NO ^c	1.58×10^{-5}	106.4	+20	+7.1	this work
DMSO ^c	7.5×10^{-5}	110.0	+46.0		41
<i>N</i> -Mepz ⁺ ^e	2.8×10^{-4}	115	+75	+0.9	17, 49
pz ^e	4.2×10^{-4}	110.5	+58.6	+13.0	17, 49
his ^c	5.3×10^{-4}	105.4	+46.0		42
2-Mepz ^e	7.7×10^{-4}	114	+44	+19.4	50
4-CNpy ^e	1×10^{-3}	105	+50	+20.6	50
py ^e	1.1×10^{-3}	103.8	+46.0		17
3,5-Me ₂ py ^e	1.2×10^{-3}	108	+60	+20.5	17, 51
3-CNpy ^e	2.2×10^{-3}	93	+16	+20.6	51
NO ₂ ^{-c}	1×10^{-2}	97	+42	+20.1	52
NH ₃ ^c	1.75×10^{-2}	102	+68	+16.4	18a, 25

^a $T = 25.0$ °C. ^b Estimated number, measured using pz as a scavenger.
^c $I = 0.1$ M. ^d Extrapolated from data reported at higher temperatures. ^e $I = 0.5$ M.

The reported activation volume is appreciably smaller for NO than for the release of other ligands, which span a range +13 to +24 cm³ mol⁻¹, but is still indicative of a dissociative mechanism. A more detailed discussion of the observed volume effects in terms of the overall volume profile for reaction 2 is presented in subsequent paragraphs.

These results all suggest that the release of NO can be described by a dissociative mechanism. Scheme 1 can also be used for this analysis by starting with reaction 7 (in a reversed manner), followed by reaction 5 and the final rapid coordination of cyanide in reaction 9.



- (48) Legros, J. J. *Chim. Phys. Phys.-Chim. Biol.* **1964**, 61, 909.
 (49) Alsheri, S.; Burgess, J. *Inorg. Chim. Acta* **1991**, 181, 153.
 (50) Sullivan, T. R.; Stranks, D. R.; Burgess, J.; Haines, R. I. *J. Chem. Soc., Dalton Trans.* **1977**, 1460.
 (51) Blandamer, M. J.; Burgess, J.; Morcom, K. W.; Sherry, R. *Transition Met. Chem.* **1983**, 8, 354.
 (52) Stochel, G.; van Eldik, R.; Hejmo, E.; Stasicka, Z. *Inorg. Chem.* **1988**, 27, 2767–2770.
 (53) Bal Reddy, K.; van Eldik, R. *Inorg. Chem.* **1991**, 30, 596–598.

Under steady-state conditions applied to the dissociative mechanism, it follows that k_{obs} , the first-order rate constant for the decay of the nitrosyl complex, will increase with increasing concentration of the scavenger ligand, cyanide, up to the point where a saturation rate constant is reached,¹⁵ i.e., where k_{-7} in Scheme 1, the rate constant for the release of NO, becomes rate-limiting. Because of the complications introduced by reaction 3, a detailed study over a wide range of cyanide concentrations could not be performed. However, within the cyanide concentration range 3–60 mM, a constant value of k_{obs} was obtained, indicating that saturation conditions were met. It is useful to compare the value of k_{-2} with those for the release of other ligands by the pentacyanoferrate(II) fragment (see Table 5). It can be seen that NO is released significantly more slowly than several other ligands affording different σ – π bonding interactions with iron. The rate is comparable with S-bonded DMSO, but it is much faster than the values obtained for the release of cyanide or CO. This suggests that the NO ligand binds to the pentacyanoferrate(II) fragment through the onset of a moderate σ – π interaction. The existence of some (minor) degree of π interaction is supported by the intense band at 345 nm, also reported for many $[\text{Fe}^{\text{II}}(\text{CN})_5\text{L}]^{3-}$ complexes with L = *N*-heterocyclic ligands, and assigned to metal-to-ligand charge transfer (MLCT) transitions.^{6,17} Although the value of the rate constant is of the same order as that measured for the dissociation of NO in some five-coordinate ferroheme complexes, significant variations in the range from 10⁻⁵ to 10 s⁻¹ have been measured by changing the heme structure.⁵⁴ The release of NO from different Fe^{II}–NO chelate complexes also depends on the spectator ligands, with values in the range from 10 to 10³ s⁻¹.¹¹ A range of values from 5 to ca. 10⁻⁴ s⁻¹ have also been obtained for the dissociation of NO from a series of ruthenium–nitrosyl complexes.^{7,55} Much has still to be learned about the factors controlling the rate of NO dissociation in the different metal systems.⁵⁶

We now turn to a discussion of the volume profile presented for reaction 2 in Figure 5, on the basis of the activation volumes determined for k_2 and k_{-2} in Tables 2 and 4, respectively. The partial molar volume of the transition state is clearly much larger than that of either the reactant or product states, illustrating the dissociative nature of the ligand substitution process. Several volume profiles for the reversible binding of NO to different iron complexes have been reported recently,^{9,11c,57,58} and a number of them support

- (54) Bohle, D. S.; Hung, C. H. *J. Am. Chem. Soc.* **1995**, 117, 9584.
 (55) (a) Lang, D. R.; Davis, J. A.; Lopes, L. G. F.; Ferro, A. A.; Vasconcellos, L. C. G.; Franco, D. W.; Tfouni, E.; Wieraszko, A.; Clarke, M. J. *Inorg. Chem.* **2000**, 39, 2294–2300. (b) Lopes, L. G. F.; Wieraszko, A.; El-Sherif, Y.; Clarke, M. J. *Inorg. Chim. Acta* **2001**, 312, 15–22.
 (56) The release of a spectator ligand from $\{\text{MNO}\}^7$ complexes (as in eq 3) is a manifestation of the strong *trans*-effect resulting from the partial population of the d_{z²} orbital by the unpaired electron derived from the nitrosyl ligand (see text for the spin distribution in $[\text{Fe}(\text{CN})_5\text{NO}]^{3-}$).³⁴ The prior release of a spectator ligand has also been observed during the studies of NO release from several *trans*- $[\text{Ru}(\text{NH}_3)_4(\text{X})(\text{NO})]^{n+}$ complexes, with X = his, ImN, ImC, H₂O, P(OEt)₃, and *N*-heterocyclic ligands.^{7,55} It has been proposed that the k_{-2} values depend on the magnitude of the *trans*-effect exerted by X.⁷

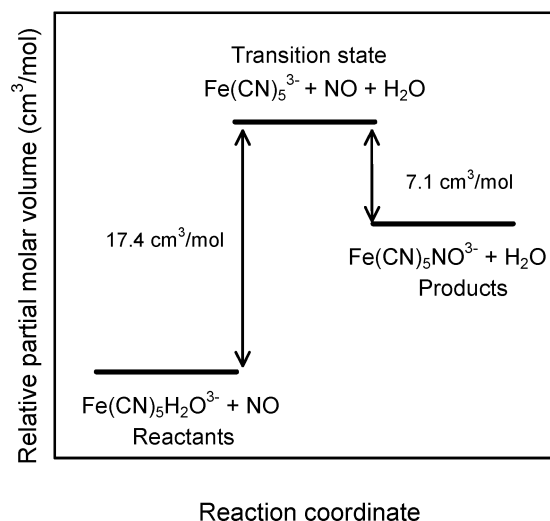


Figure 5. Volume profile for overall reaction 2.

the operation of a dissociative mechanism.^{9,11c,57,58} A direct comparison of the reactions of NO with $[\text{Fe}(\text{H}_2\text{O})_6]^{2+}$ and $[\text{Fe}(\text{CN})_5\text{H}_2\text{O}]^{3-}$ indicates that both the complex-formation and release of NO reactions are accompanied by significantly larger activation volumes for the latter system.⁹ This underlines our claim that the reactions involving the pentacyano complex are more dissociative in character than those involving the hexaaqua complex, for which a dissociative interchange mechanism was suggested.⁹ The overall reaction volume for reaction 2 in Figure 5, viz. $+10.3 \pm 0.5 \text{ cm}^3 \text{ mol}^{-1}$, is also more positive than the value of $+4.8 \pm 0.6 \text{ cm}^3 \text{ mol}^{-1}$ reported for the hexaaquairon(II) system.⁹ This may be partially due to the formal change in oxidation state when $[\text{Fe}(\text{H}_2\text{O})_6]^{2+}$ reacts with NO to produce $[\text{Fe}^{\text{III}}(\text{H}_2\text{O})_5(\text{NO})]^{2+}$ as compared to the formation of $[\text{Fe}^{\text{II}}(\text{CN})_5\text{NO}]^{3-}$ in the case of the pentacyano complex.⁹ Other examples where the volume profiles clearly supported the operation of a limiting dissociative mechanism are for the reaction of NO with metmyoglobin⁵⁸ and a series of iron(III) porphyrin complexes.⁵⁷ In the latter case, it was shown that the rate and mechanism of the binding of NO are controlled by the water exchange process on the porphyrin complexes.⁵⁹

The limiting dissociative mechanism suggested for reaction 2 is also in line with that expected on the basis of the σ -donor and π -acceptor properties of the cyano ligands that will cause significant *cis* and *trans* labilization effects in terms of the displacement of coordinated water or NO.²⁵ It is important that the volume profile reported in Figure 5 is the first one for a reversible complex-formation reaction with NO that does not involve a formal oxidation or reduction of the metal center as is the case for all other volume profiles reported so far.^{9,11c,57,58,60}

(57) Laverman, L. E.; Hoshino, M.; Ford, P. C. *J. Am. Chem. Soc.* **1997**, *119*, 12663–12664.

(58) Laverman, L. E.; Wanat, A.; Oszejka, J.; Stochel, G.; Ford, P. C.; van Eldik, R. *J. Am. Chem. Soc.* **2001**, *123*, 285–293.

(59) Schnepfensieper, T.; Zahl, A.; van Eldik, R. *Angew. Chem., Int. Ed.* **2001**, *40*, 1678–1680.

(60) It should be kept in mind that some charge transfer from NO to Fe(II) does occur and spin density calculations indicate that 35% of the unpaired electron is located on iron, although we can still approach this description as $\text{Fe}^{\text{II}}\text{--NO}$.³⁴

A remarkable aspect of the volume profile reported in Figure 5 is the fact that the volume of activation for the formation of the transition state is significantly larger than that predicted for the dissociation of a water molecule from an octahedral hexaaqua complex, viz. $+13 \text{ cm}^3 \text{ mol}^{-1}$.⁴⁶ A very large and similar volume of activation was also reported for the reaction between $[\text{Fe}(\text{CN})_5\text{H}_2\text{O}]^{3-}$ and ammonia studied before.²⁵ In the present case, the volume increase almost equals the partial molar volume of a bulk solvent (water) molecule, which means that no major volume collapse during the reorganization of the five-coordinate $[\text{Fe}(\text{CN})_5]^{3-}$ intermediate occurs, as was predicted for the pentaqua intermediate.⁴⁶ This may be related to the highly solvated nature of the pentacyano fragment in a polar solvent like water, which could prevent significant ligand reorganization on going from a six- to a five-coordinate state. Furthermore, the volume of activation for the release of NO in the back reaction is rather surprisingly small (compared to all the other volume of activation data reported in Table 5), which may indicate that specific solvation effects around the NO radical on its release from the coordination sphere could partially compensate the intrinsic volume increase associated with $\text{Fe}^{\text{II}}\text{--NO}$ bond cleavage. Thus, the volume profile for the rather unique reversible binding of NO to pentacyanoferrate(II) that involves only a minor charge transfer from NO to the Fe(II) center³⁴ reveals some interesting features not observed in related volume profiles reported before and calls for further investigations on similar or related systems.

Conclusions

In contrast to the behavior found for the interaction of $[\text{Fe}^{\text{III}}(\text{CN})_5\text{H}_2\text{O}]^{2-}$ with NO in which the complex was first reduced by NO prior to coordination, the interaction of NO with $[\text{Fe}^{\text{II}}(\text{CN})_5\text{H}_2\text{O}]^{3-}$ shows that NO behaves as a common Lewis base. Since the complex-formation rate constant is controlled by the dissociation of water, no specific information on the coordination properties of NO can be obtained from the kinetic experiments. Furthermore, no specific influence of the unpaired electron on NO can be disclosed, as compared to the coordination ability of diamagnetic ligands. The rate law and activation parameters support the operation of a limiting dissociative mechanism, as found for complex-formation reactions with other nucleophiles. The release of NO is also governed by a dissociative mechanism, revealing that NO binds to pentacyanoferrate(II) through the onset of moderate to strong $\sigma\text{--}\pi$ interactions, as suggested by the low value of k_{-2} . By comparison with the release of NO^+ as a ligand in NP, NO dissociates much faster (the dissociation of NO^+ is presently undetectable in $\text{M}^{\text{II}}\text{NO}^+$ complexes). Although NO should be a stronger Lewis base than NO^+ , it should also be a much weaker π -acceptor. In view of the reported value for k_{-2} , it is feasible that NO is not released through the dissociation of NO from $[\text{Fe}(\text{CN})_5\text{NO}]^{3-}$ following biological reduction of NP, but rather through decomposition routes involving the decay of the tetracyanonitrosyl complex as suggested. This aspect is presently under further investigation.

Acknowledgment. The authors gratefully acknowledge financial support from the Deutsche Forschungsgemeinschaft and the Volkswagen Foundation, as well as from the University of Buenos Aires and the Argentinian agencies ANPCyT and Conicet. J.A.O. is a member of the scientific staff, and F.R. is a fellow of Conicet. We appreciate the

assistance of Manfred Pöhlein (University of Erlangen-Nürnberg) with the GC-MS measurements.

Supporting Information Available: Additional figures. This material is available free of charge via the Internet at <http://pubs.acs.org>.

IC0342189